J Mater Sci (2008) 43:4198–4207
DOI 10.1007/s10853-008-2602-5

Synthesis of lamellar mesostructured calcium phosphates using *n*-alkylamines as structure-directing agents in alcohol/water mixed solvent systems

Nobuaki Ikawa · Yasunori Oumi · Tatsuo Kimura · Takuji Ikeda · Tsuneji Sano

Received: 25 November 2007 / Accepted: 20 March 2008 / Published online: 10 April 2008

Abstract Lamellar mesostructured calcium phosphates constructed by ionic bonds were prepared by using *n*-alkylamines (*n*-$C_nH_{2n+1}NH_2$, $n = 8$–18) at room temperature in the mixed solvent systems of aliphatic alcohol ($C_nH_{2n+1}OH$, $n = 1$–4) and water, and the synthetic conditions were investigated in detail. The mixed solvent systems suppressed the formation of crystalline calcium phosphates like brushite ($CaHPO_4{\cdot}2H_2O$) and monetite ($CaHPO_4$) at low temperatures, successfully affording pure lamellar mesostructured calcium phosphates. Other crystalline phases such as hydroxyapatite ($Ca_{10}(PO_4)_6(OH)_2$) were not formed under the conditions with the Ca/P molar ratios in the range of 0.7–1.0 in the starting mixtures. The Ca/P molar ratio of the lamellar mesostructured calcium phosphates was ca. 1.0, calculated by ICP and ^{31}P MAS NMR data. Interestingly, the kind of alcohols strongly influenced the solubilities of calcium phosphate species and *n*-alkylamines, and then lamellar mesostructured phases were obtained with some morphological variation.

N. Ikawa · Y. Oumi · T. Sano (✉)
Department of Applied Chemistry, Graduate School of Engineering, Hiroshima University, Higashi-Hiroshima 739-8527, Japan
e-mail: tsano@hiroshima-u.ac.jp

T. Kimura
National Institute of Advanced Industrial Science and Technology (AIST), Shimoshidami, Moriyama-ku, Nagoya 463-8560, Japan

T. Ikeda
AIST, Tohoku, Nigatake, Miyagino-ku, Sendai 983-8551, Japan

Introduction

Ordered mesoporous materials have been prepared by using amphiphilic organic molecules which are self-organized in aqueous solutions, and their hydrophilic headgroups are interacted with soluble inorganic species [1–4]. Surfactant-templated mesoporous materials have some specific features such as high surface areas and high adsorption capacities including the uniformity and periodicity of tunable mesopores [5–7], which are widely applicable to adsorbents and catalytic supports [8–11]. Crystalline calcium phosphates used as adsorbents have showed surface areas lower than 100 $m^2\ g^{-1}$ so far. The value is obviously inferior to those of periodic mesoporous materials [12–14]. Recently, bioactive mesoporous silica whose surfaces are covered with apatite layers grown in simulated body fluid is reported as a high capacity vessel for drug delivery and scaffold materials [15]. The paper suggests the potential application of mesoporous calcium phosphates as biomaterials.

Synthetic procedures of ordered mesoporous materials have mainly been advanced for controlling mesostructure [16, 17] and pore size through the investigation on silica-based materials, as well as compositional variations of the frameworks [18–22]. Inorganic-organic mesostructured composites, which are formed by the self-assembly of surfactant molecules attached with soluble inorganic species and condensation of the inorganic species, act as precursors of ordered mesoporous materials [5–7]. Surfactant-templating has applied to the synthesis of other mesoporous inorganic solids such as metal oxides and phosphates [18–36]. However, it is quite difficult to synthesize surfactant-templated mesoporous materials composed of pure calcium phosphates because the inorganic frameworks are strongly connected through ionic

bonds between calcium and phosphate ions. Some research groups have only commented the possibility to form lamellar mesostructured calcium phosphates [37–42]. In general, it is recognized that calcium phosphate-based materials with ionic frameworks are more preferential to be crystallized than other covalently bonded metal phosphates. Actually, in the previous reports on the synthesis of mesostructured calcium phosphates using surfactants, it is difficult to suppress the crystallization of calcium phosphate species for obtaining mesostructured precursors composed of calcium phosphates except for lamellar phases. In addition, the formation of the lamellar phases has not been proved by TEM so far.

Recently, we have developed the synthetic method of lamellar mesostructured calcium phosphate by using *n*-hexadecylamine in the mixed solvent system of ethanol and water, which suppresses the crystallization and controls the solubility of calcium phosphate species [43]. In the present study, we investigated the effects of the synthetic conditions such as alcohol/water molar ratio, Ca/P molar ratio, reaction temperature, the kind of alcohol, and the alkyl chain length of *n*-alkylamine in more detail on the formation of lamellar mesostructured calcium phosphates.

Experimental

Materials

All the *n*-alkylamines (n-$C_nH_{2n+1}NH_2$, $n = 8$, 10, 12, 16, and 18) were obtained from Tokyo Kasei Kogyo Co. Phosphoric acid (85% H_3PO_4), aqueous solution of ammonia (25% NH_3), and calcium acetate monohydrate ($Ca(OAc)_2{\cdot}H_2O$) were obtained from Wako Chemical Co. Aliphatic alcohols such as methanol (MeOH), ethanol (EtOH), *n*-propanol (PrOH), and *n*-butanol (BuOH) were also purchased from Wako Chemical Co. and used without further purification. Calcium hydroxide ($Ca(OH)_2$) was obtained from Kanto Chemical Co.

Synthesis of mesostructured calcium phosphate

Lamellar mesostructured calcium phosphate was prepared as follows. n-$C_nH_{2n+1}NH_2$ and 85% H_3PO_4 were added to a mixed solvent of alcohol and water. A white slurry was obtained after stirring over 1 h. $Ca(OAc)_2{\cdot}H_2O$ and 25% NH_3 were then added to the white slurry under vigorous stirring and the stirring was maintained for 15 min. The starting mixture ($Ca(OAc)_2$:H_3PO_4:n-$C_nH_{2n+1}NH_2$:0.5NH_3:40n-$C_nH_{2n+1}OH$:40H_2O) was statically kept for another 5 days at room temperature. The product was filtered, washed with EtOH repeatedly, and air-dried.

Characterization

X-ray diffraction (XRD) patterns were obtained by using a Rigaku RINT 2000 with graphite monochromatized Cu-Kα radiation (40 kV, 30 mA). The compositions were measured by using an inductively coupled plasma atomic emission spectroscopy (ICP-AES, Seiko SPS 7700). Thermogravimetric (TG) analysis was conducted by using a Seiko TG/DTA320 thermal analyzer. Transmission electron microscopic (TEM) images were taken by a JEOL JEM-2010 microscope, operated at 200 kV. ^{31}P MAS NMR spectra were obtained by using a Bruker DRX-400 spectrometer with a 7 mm zirconia rotor at a resonance frequency of 161.9 MHz with a spinning rate of 6 kHz. The spectra were accumulated with 4.5 μs pulses and 40 s recycle delay. An aqueous solution of H_3PO_4 (85%) was used as a chemical shift reference. ^{13}C CP/MAS NMR spectra were also collected by using the same spectrometer at 100.7 MHz with a spinning rate of 4 kHz, 6.8 μs pulses, and 15 s recycle delay. Tetramethylsilane was used as a chemical shift reference. Scanning electron microscopic (SEM) images were taken by a JEOL JSM-6320FS.

Results and discussion

The crystallization of calcium phosphate species formed through rapid reaction between calcium and phosphate ions is dramatically faster than other inorganic compounds constructed by covalent bonds. Indeed, there are few reports on the preparation of amorphous calcium phosphates that must exist before transformation into stable crystalline phases [44]. Since interaction between surfactant molecules and phosphate ions is lost by the formation of discrete crystalline calcium phosphates, it is necessary to control mesostructures of calcium phosphates before the rapid formation of crystalline calcium phosphates. Accordingly, we have suggested a two-step reaction; alkylammonium phosphates are utilized as intermediates [45], followed by the reaction with calcium sources under conditions that keep ionic bonds between alkylammonium and phosphate ions during the generation of mesostructured calcium phosphates.

Effect of EtOH/H_2O molar ratio

The synthesis of lamellar mesostructured calcium phosphate using n-$C_{16}H_{33}NH_2$ was carried out in the mixed solvent of ethanol (EtOH) and water. The starting mixtures were prepared by mixing 85% H_3PO_4, $Ca(OAc)_2{\cdot}H_2O$ and 25% NH_3 in the mixed solvent with different molar ratios of EtOH to water. The composition of the starting mixtures was $Ca(OAc)_2$:H_3PO_4:n-$C_{16}H_{33}NH_2$:0.5NH_3:80(EtOH + H_2O).

The XRD patterns of the products prepared in the presence and absence of n-$C_{16}H_{33}NH_2$ are shown in Fig. 1. Even when the synthesis was conducted in the presence of n-$C_{16}H_{33}NH_2$, a hydrated product such as brushite ($CaHPO_4{\cdot}2H_2O$) was mainly obtained in the aqueous system (Fig. 1A(a)) [46]. Brushite was also formed in the absence of the surfactant in the aqueous system (Fig. 1B(a)). With the increase in the amount of EtOH in the reaction systems containing n-$C_{16}H_{33}NH_2$, the peaks due to brushite disappeared (Fig. 1A(b–d)), indicating that the formation of brushite is suppressed in the EtOH/H_2O systems. The synthesis of crystalline calcium phosphates in the EtOH/H_2O systems without surfactants was already reported and the preferential formation of brushite is suppressed by EtOH as a co-solvent [47]. Therefore, similar synthesis was conducted without the surfactant. Peaks due to brushite disappeared gradually with the increase in the amount of EtOH (Fig. 1B(a–d)). Alternatively, peaks due to monetite ($CaHPO_4$) that is one of anhydrous calcium phosphate phases appeared by increasing the amount of EtOH (Fig. 1B(c–e)). In contrast, a peak with the d-spacing of 4.5 nm and the higher order diffractions, that are assignable to lamellar phases, appeared in low diffraction angles for the product obtained in the similar reaction systems containing n-$C_{16}H_{33}NH_2$ (Fig. 1A(b–d)). The formation of lamellar mesostructured calcium phosphates was confirmed by TEM, showing clear striped patterns (Fig. 2). The results reveal that the lamellar mesostructured calcium phosphate can be obtained in the mixed solvent systems [43]. It is considered that further increase of the amount of EtOH is not useful for the reaction between $Ca(OAc)_2$ and H_3PO_4 because $Ca(OAc)_2{\cdot}H_2O$ cannot be dissolved in the mixtures (Fig. 1A(e) and B(e)). Accordingly, only lamellar hexadecylammonium phosphate [(n-$C_{16}H_{33}NH_3^+$)($H_2PO_4^-$)] is formed in the ethanolic system containing n-$C_{16}H_{33}NH_2$ (Fig. 1A(e)).

Effect of Ca/P molar ratio

Lamellar mesostructured calcium phosphates were synthesized under the conditions with different Ca/P molar ratios in the starting mixtures. The composition of the starting mixtures was 0.7–1.5$Ca(OAc)_2$:H_3PO_4:n-$C_{16}H_{33}NH_2$:0.5NH_3:80(EtOH + H_2O). The EtOH/H_2O molar ratio was simultaneously changed with the variation in the Ca/P molar ratio under the condition with the fixed H_2O/Ca molar ratio (40) in the reaction system. The XRD patterns of the products obtained at the Ca/P molar ratios of 0.7–1.5 in the starting mixtures are shown in Fig. 3. In the products obtained at the Ca/P molar ratios ranging from 0.7 to 1.0, the peaks observed at $2\theta = 1.5$–$6.0°$ are corresponded to the formation of lamellar mesostructured calcium phosphate ($d_{001} = 4.5$ nm) (Fig. 3A(a–c)). Several peaks, which are not assignable to crystalline calcium phosphates, were also observed in high diffraction angles (Fig. 3B(a–c)). Some of the peaks are considered to be due to the ordering in the calcium phosphate framework of the lamellar phase. However, the assignment of the peaks has not been achieved yet because of the broadening of the peaks due to distortion of the layered structure. With the further increase in the Ca/P molar ratio from 1.2 to 1.5, peaks at $2\theta = 15$–$25°$ (Fig. 3B(d–e)) as well as the peaks assignable to the lamellar mesostructured calcium phosphate disappeared (Fig. 3A(d–e)) although small broad

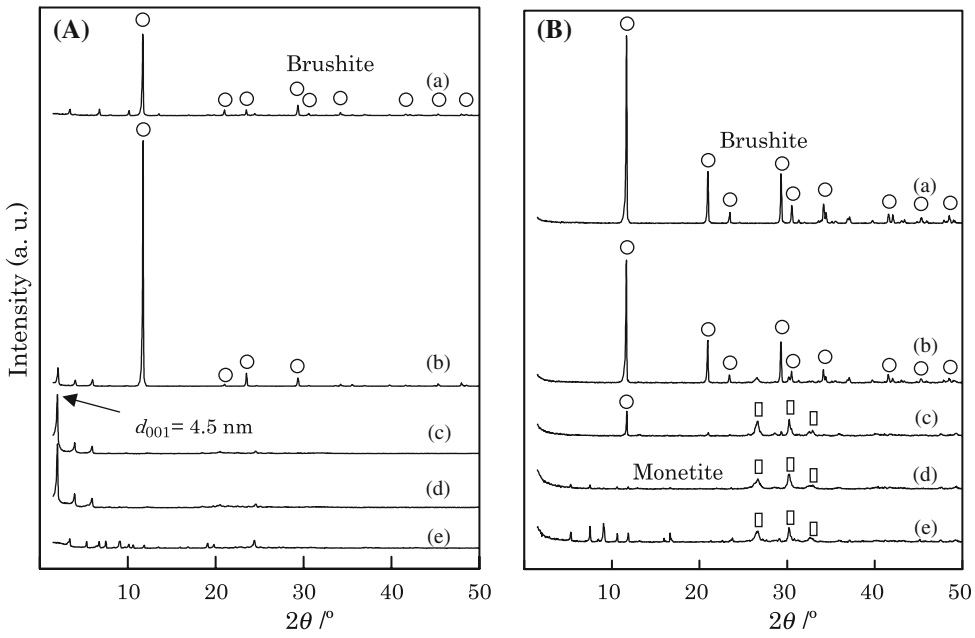

Fig. 1 XRD patterns of the products obtained (**A**) with and (**B**) without $C_{16}H_{33}NH_2$. EtOH/H_2O ratio: (a) 0/100, (b) 25/75, (c) 50/50, (d) 75/25, and (e) 96/4

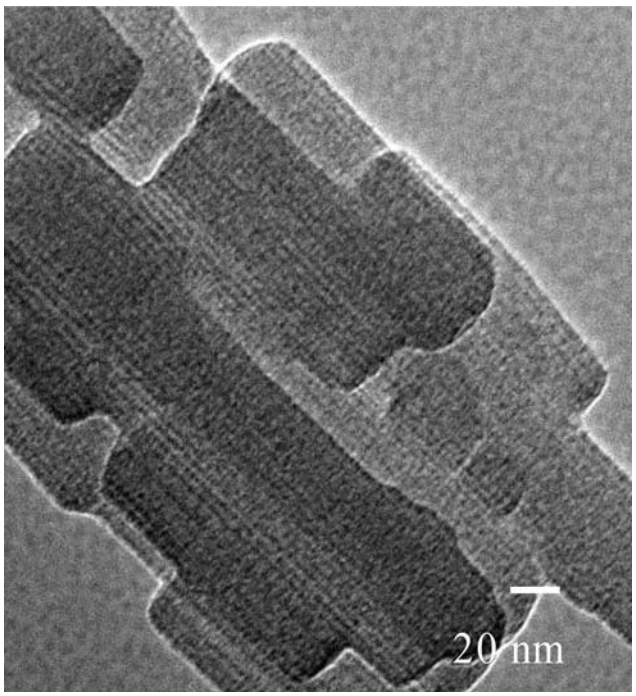

Fig. 2 TEM image of lamellar mesostructured calcium phosphate obtained with EtOH/H_2O (50/50)

peaks assignable to initial crystalline hydroxyapatite phase appeared at $2\theta = 26°$ and 32° (Fig. 3B(d–e)) [44, 48]. The result indicates that the formation of the lamellar mesostructured calcium phosphate occur at the Ca/P molar ratios from 0.7 to 1.0 because the hydroxyapatite phase is formed preferentially at higher Ca/P molar ratios than 1.0. Hydroxyapatite ($Ca_{10}(PO_4)_6(OH)_2$) known as anhydrate crystalline calcium phosphate was formed in the non-aqueous solvent system under the calcium-rich conditions. When the composition of the starting mixture was changed into $0.7Ca(OAc)_2$:H_3PO_4:*n*-$C_{16}H_{33}NH_2$:$0.5NH_3$:40EtOH:$40H_2O$, lamellar mesostructured calcium phosphate was obtained with the formation of the small amount of brushite. The result would be caused from the H_2O-rich condition (H_2O/Ca molar ratio of 40/0.7) because the presence of H_2O in the reaction system is necessary for controlling the dissolution of the calcium source.

The ^{31}P MAS NMR measurements were applied to get further information on the calcium phosphate frameworks and the spectra of the products prepared by changing the Ca/P molar ratios in the range of 0.7–1.5 in the starting mixtures are shown in Fig. 4. In the ^{31}P MAS NMR spectrum of the product obtained at Ca/P = 0.7, three peaks were observed at 2.1, 0.4, and −1.7 ppm (Fig. 4b). In compared with the spectrum of (n-$C_{16}H_{33}NH_3^+$)($H_2PO_4^-$) (Fig. 4a), the small peak at 0.4 ppm is considered to be assigned to P atoms in the similar salt. With the increase in the Ca/P molar ratio, the intensity of the shoulder peak at around −1.7 ppm decreased gradually while that of the peak at 2.1 ppm was enhanced (Fig. 4b–e). The ^{31}P MAS NMR spectra were also measured with ^{1}H–^{31}P cross-polarization (CP) technique (not shown here). The intensity of the peak at 2.1 ppm was not enhanced in the ^{31}P CP/MAS NMR spectrum, being consistent with the lack of protons close to P atoms in the calcium phosphate framework. However, the CP enhancement was observed for the product obtained at Ca/P = 0.9, revealing the presence of two PO_4 units, probably, $[\mathbf{P}O_4]^{3-}$ and $[\mathbf{H}PO_4]^{2-}$ or $[H_2\mathbf{P}O_4]^-$, in the framework of the lamellar mesostructured calcium phosphate [49, 50].

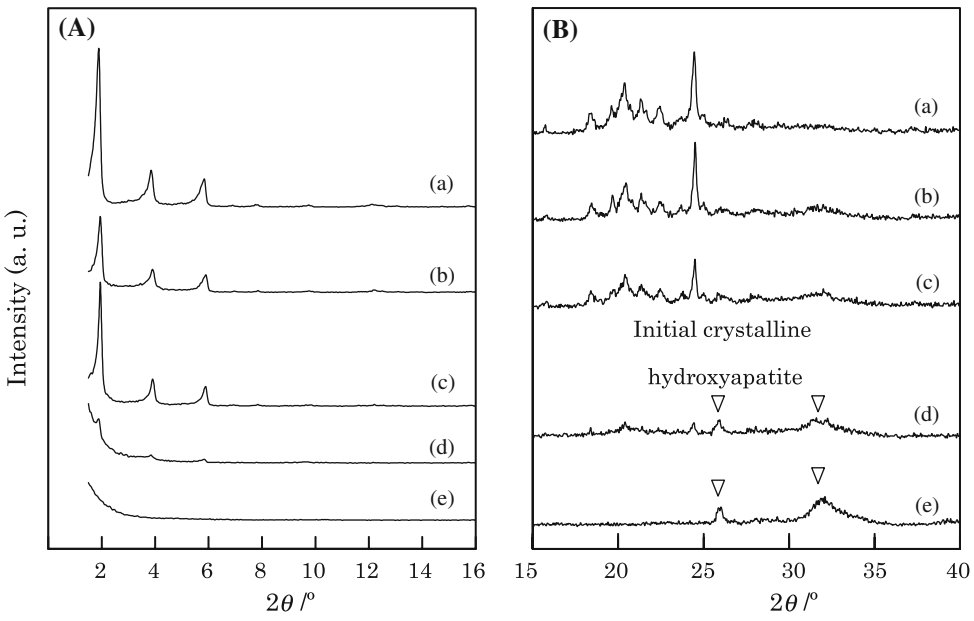

Fig. 3 XRD patterns at (**A**) low and (**B**) high angles of the products obtained at various Ca/P ratios: (a) 0.7, (b) 0.9, (c) 1.0, (d) 1.2, and (e) 1.5

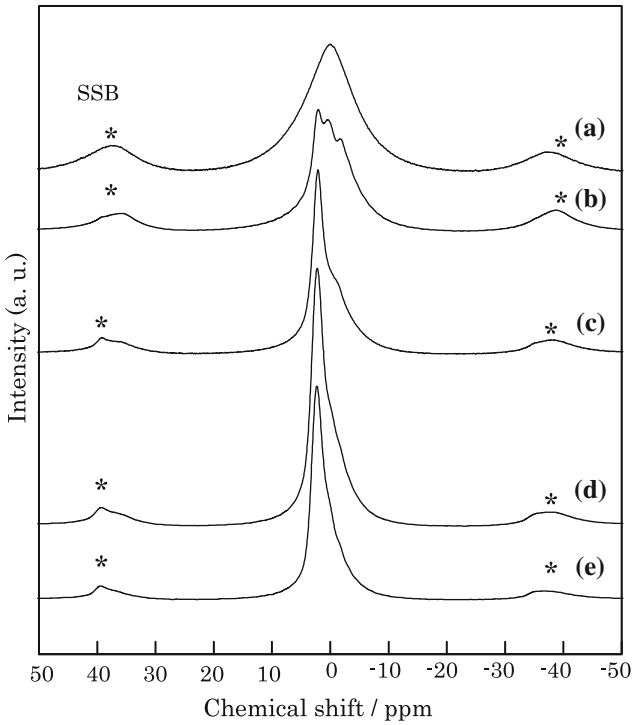

Fig. 4 ^{31}P MAS NMR spectra of lamellar mesostructured calcium phosphates obtained at different Ca/P ratios: (a) [$C_{16}H_{33}NH_3^+$] [$H_2PO_4^-$], (b) 0.7, (c) 0.9, (d) 1.0, and (e) 1.2

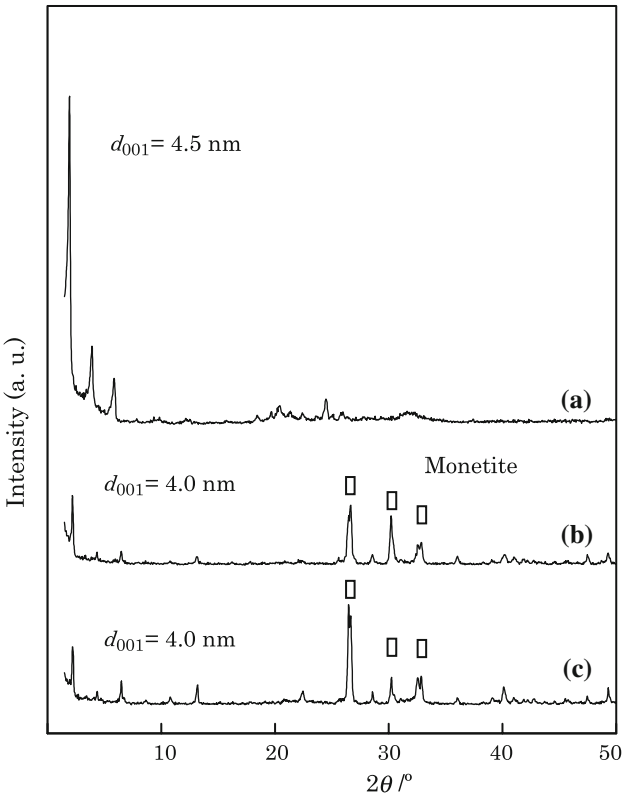

Fig. 5 XRD patterns of the products prepared at (a) room temperature, (b) 50 °C, and (c) 70 °C

Effect of the reaction temperature

The synthesis was conducted at different temperatures under the condition with the composition of $Ca(OAc)_2$:H_3PO_4:*n*-$C_{16}H_{33}NH_2$:0.5NH_3:40EtOH:40H_2O. After the starting mixture was stirred for 15 min, the mixture was aged at room temperature, 50 °C, and 70 °C statically. The XRD patterns of the products are shown in Fig. 5. Although all the XRD patterns showed the formation of lamellar mesostructured calcium phosphates, the d_{001} values (4.0 nm) of the lamellar phases obtained at 50 °C and 70 °C were smaller than that of the lamellar phase (4.5 nm) prepared at room temperature (Fig. 5a–c). In addition, the products obtained by heating contained monetite as a byproduct and the amount of the byproduct was increased by elevating the synthetic temperature [51]. None of typical striped patterns characteristic for lamellar mesostructured materials were found in the TEM images of the products obtained at 50 °C and 70 °C. After each product (0.5 g) was stirred at 60 °C for 5 h in EtOH (150 g), filtered, and washed with EtOH at 60 °C, only the peaks in the low diffraction angles disappeared completely. It is reasonable to be considered that this phase is not a lamellar phase but would be self-assembled organic molecules, probably a moiety of *n*-$C_{16}H_{33}NH_2$ and/or (*n*-$C_{16}H_{33}NH_3^+$) ($H_2PO_4^-$). The formation of monetite would be more preferential to occur at high temperatures than that of the lamellar mesostructured calcium phosphate.

The synthetic regions where several calcium phosphates can be obtained under the conditions with various EtOH/H_2O and Ca/P molar ratios at room temperature are schematized in Fig. 6. In the region of Ca/P molar ratios higher than 1.0, the formation of hydroxyapatite predominantly occurs in the mixed solvent system regardless of the EtOH/H_2O molar ratio. When the Ca/P molar ratios are lower

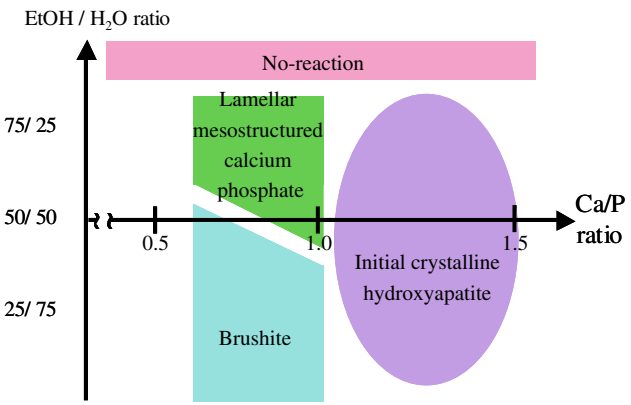

Fig. 6 Phase diagram of calcium phosphates prepared in the presence of *n*-$C_{16}H_{33}NH_2$ at room temperature

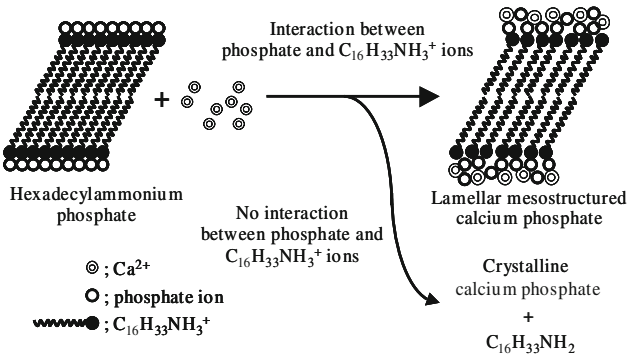

Fig. 7 Proposed formation route of lamellar mesostructured calcium phosphate

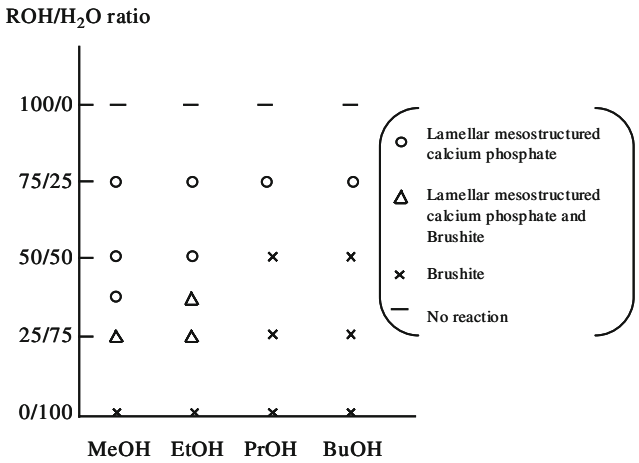

Fig. 8 Effect of aliphatic alcohol on the synthesis of lamellar mesostructured calcium phosphate using *n*-$C_{16}H_{33}NH_2$

than 1.0, brushite is formed in the H_2O-rich system. The reaction between (*n*-$C_{16}H_{33}NH_3^+$)($H_2PO_4^-$) and calcium source does not occur in the pure EtOH system. Monetite is formed during the aging at high temperatures. This result strongly indicates that the interaction between hexadecylammonium and phosphate ions is necessary to obtain the lamellar mesostructured calcium phosphate during the reaction of calcium ions and hexadecylammonium phosphate (Fig. 7).

Effect of alcohol as co-solvent

Effect of co-solvents was investigated in the presence of a series of aliphatic alcohols. The composition of the starting mixtures was $Ca(OAc)_2$:H_3PO_4:*n*-$C_{16}H_{33}NH_2$:0.5NH_3:80(ROH + H_2O), R = CH_3, C_2H_5, C_3H_7, and C_4H_9. The ROH/H_2O molar ratio was changed from 0/100 to 96/4. The mixture of lamellar mesostructured calcium phosphate and brushite was obtained at the MeOH/H_2O molar ratio of 25/75. The formation of brushite was suppressed with the increase in MeOH, leading to the successful formation of pure lamellar phase in the range of the MeOH/H_2O molar ratio from 40/60 to 75/25. In the PrOH/H_2O and BuOH/H_2O systems, pure lamellar mesostructured calcium phosphates were obtained at ROH/H_2O of 75/25, and only brushite was formed under the conditions in the range of the ROH/H_2O molar ratio from 50/50 to 25/75. Accordingly, the formation of brushite was suppressed by increasing the amount of MeOH, PrOH, and BuOH as well as EtOH. However, there is the difference in the range of the ROH/H_2O molar ratio to afford lamellar mesostructured calcium phosphate. The results are schematically summarized in Fig. 8. Lamellar phases were formed under restricted conditions with the ROH/H_2O molar ratios in the presence of aliphatic alcohols having longer alkyl chains. Actually, the range of the EtOH/H_2O molar ratio affording pure lamellar mesostructured calcium phosphate was narrower than that of the MeOH/H_2O molar ratio. As ROH with longer alkyl chains is not mixed with H_2O because hydrophobicity of the alcohol becomes strong, the reaction system seems to be analogous to aqueous systems, which has a tendency to provide hydrated crystalline calcium phosphate phases such as brushite. Therefore, the effective range of the ROH/H_2O molar ratio becomes narrow with an increase in the alkyl chain length of alcohol, which prevents the formation of lamellar mesostructured calcium phosphate. The results indicate that the kind of alcohol is important for controlling the solubility of the calcium source and the preferential formation of crystalline calcium phosphate phases.

The TEM images of the mesostructured calcium phosphates obtained under the conditions with the ROH/H_2O molar ratios of 75/25 and 50/50 in the presence of a series of ROH are shown in Fig. 9. Stripe patterns were clearly observed for all the products obtained at ROH/H_2O of 75/25 (Fig. 9a, d–f). However, in addition to the stripe patterns (Fig. 9b), disordered stripe patterns were slightly observed for the product obtained at MeOH/H_2O of 50/50 (Fig. 9c). The SEM images of the products obtained at ROH/H_2O of 75/25 are shown in Fig. 10. The lamellar mesostructured calcium phosphates showed plate-like morphologies and the particle size gradually increased in the presence of ROH with longer alkyl chains, revealing that the particle size of the lamellar phases is controllable according to the alkyl chain length of alcohols in the mixed solvent systems.

Possible structure of lamellar mesostructured calcium phosphate

On the basis of the ^{31}P MAS NMR results, it is considered that the calcium phosphate frameworks contain two phosphate units. The elemental analysis showed that Ca/P molar

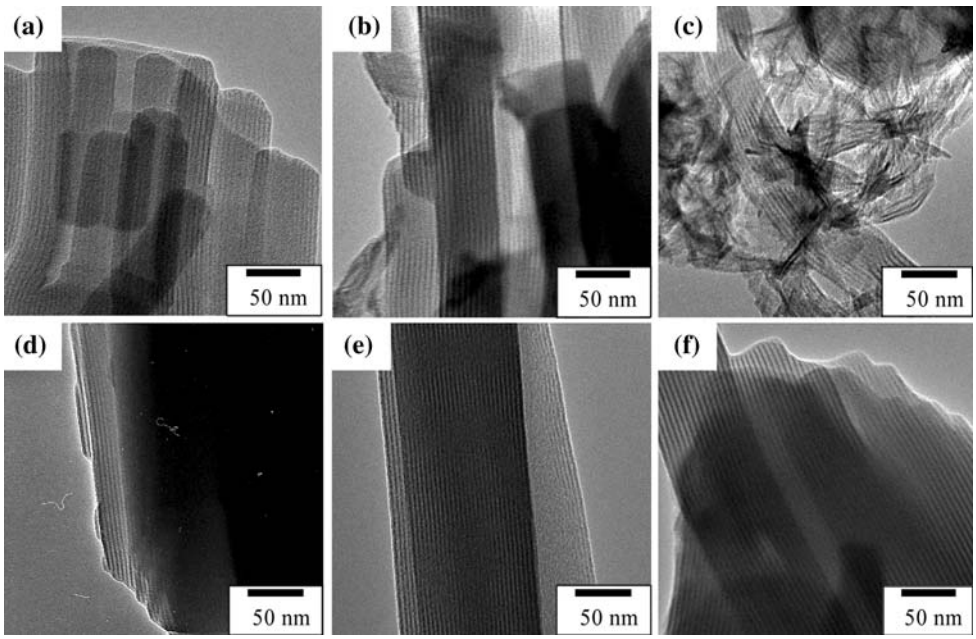

Fig. 9 TEM images of lamellar mesostructured calcium phosphates obtained in the ROH/H_2O systems. (**a**) MeOH/H_2O (75/25), (**b**) and (**c**) MeOH/H_2O (50/50), (**d**) EtOH/H_2O (75/25), (**e**) PrOH/H_2O (75/25) and (**f**) BuOH/H_2O (75/25)

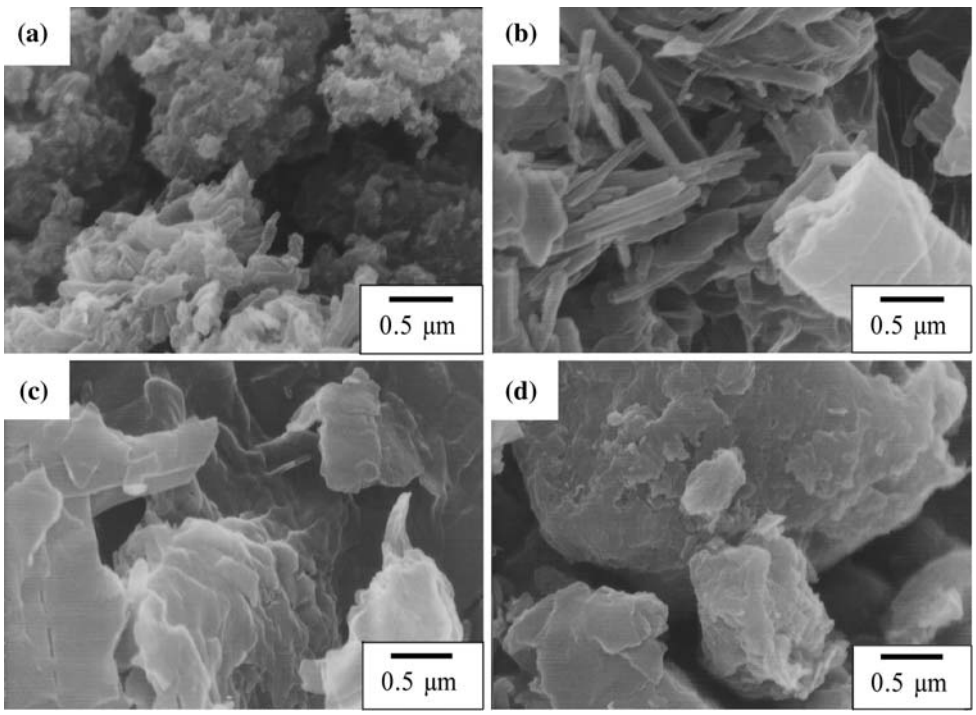

Fig. 10 SEM images of lamellar mesostructured calcium phosphates obtained in the ROH/H_2O (75/25) systems: (**a**) MeOH, (**b**) EtOH, (**c**) PrOH, and (**d**) BuOH

ratios in the frameworks were almost consistent with those in the corresponding starting mixtures. The TG curve of the lamellar mesostructured compound with the Ca/P molar ratio of 1.0 is shown in Fig. 11. Mass losses of 23.0 and 28.7 mass% were mainly observed below 200 °C and between 200 °C and 600 °C, which correspond to dehydration and combustion of organic moieties, respectively. The XRD peaks of the white solid obtained by calcination of the lamellar phase at 600 °C for 10 h were assignable to peaks due to calcium pyrophosphate ($Ca_2P_2O_7$) (Fig. 12). On the basis of the mass loss below 600 °C, the formula was presented as $(C_{16}H_{33}NH_3^+)_{0.6}Ca^{2+}(HPO_4^{2-})_{0.4}(PO_4^{3-})_{0.6}$.

Lamellar mesostructured calcium phosphates were prepared by using n-$C_nH_{2n+1}NH_2$ with different alkyl chain lengths as structure-directing agents. Calcium hydroxide was used as a calcium source instead of calcium acetate monohydrate, because the products containing both lamellar mesostructured calcium phosphate (main product) and alkylammonium phosphate salt (byproduct) were obtained by using n-$C_nH_{2n+1}NH_2$ except for n-$C_{16}H_{33}NH_2$

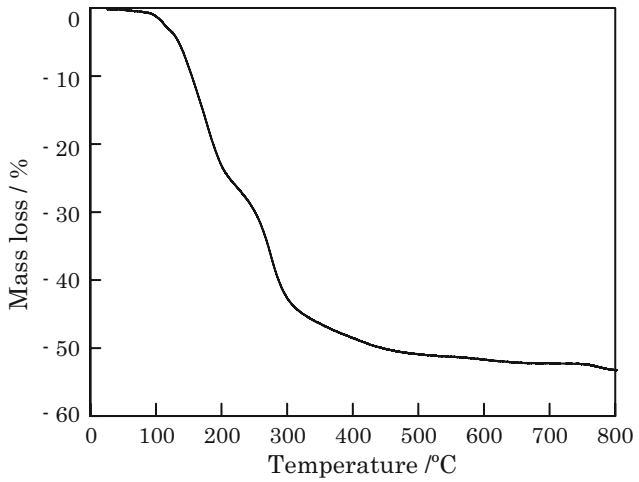

Fig. 11 TG curve of lamellar mesostructured calcium phosphate with Ca/P molar ratio of 1.0

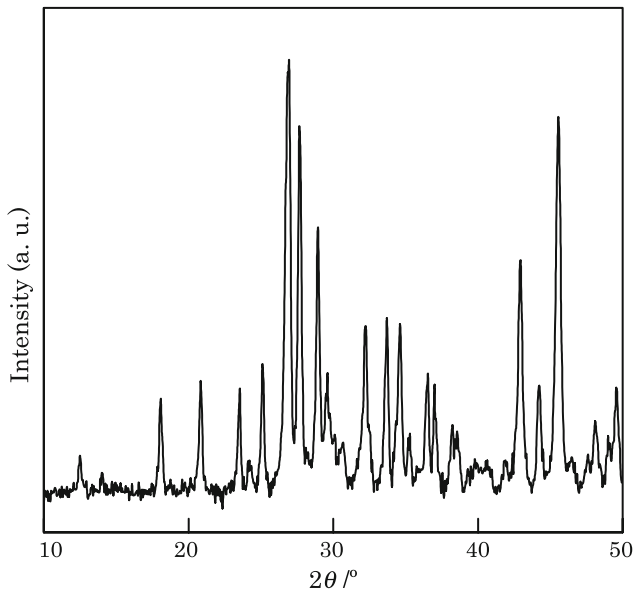

Fig. 12 XRD pattern of the calcined product of lamellar mesostructured calcium phosphate with the Ca/P molar ratio of 1.0 at 600 °C

when calcium acetate monohydrate was used. The XRD patterns of the products obtained from a series of starting mixtures with $Ca(OH)_2$:H_3PO_4:n-$C_nH_{2n+1}NH_2$ (n = 8–18):40EtOH:40H_2O are shown in Fig. 13. The patterns contained the peaks due to both unreacted calcium hydroxide and lamellar mesostructured calcium phosphate. The d_{001} values of the lamellar phases were changed in the range of 2.8–4.8 nm (2.8 nm for n = 8, 3.4 nm for n = 10, 3.7 nm for n = 12, 4.5 nm for n = 16, and 4.8 nm for n = 18). Conformation of the alkyl chains of the surfactant molecules (n-$C_{16}H_{33}NH_2$) in the lamellar mesostructured calcium phosphate was investigated by ^{13}C CP/MAS NMR. The ^{13}C CP/MAS NMR spectrum of the lamellar mesostructured calcium phosphate obtained from the

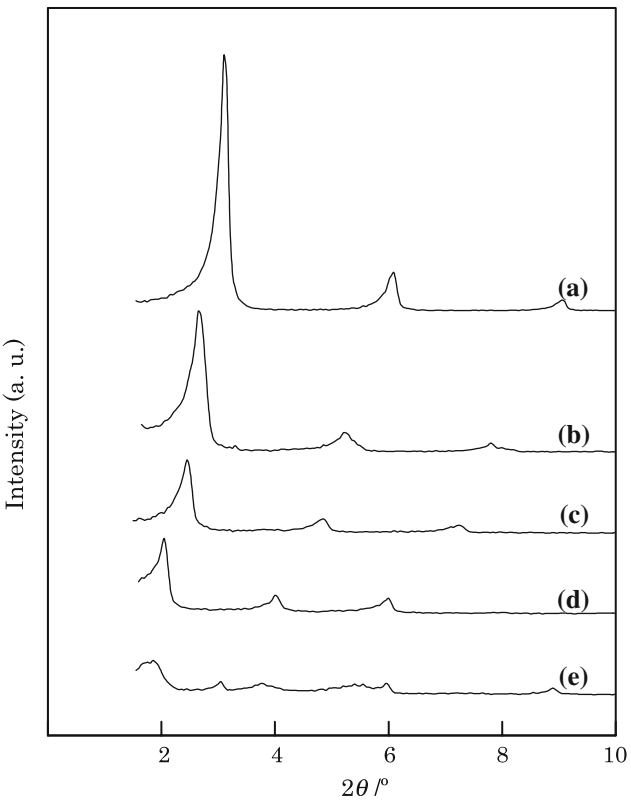

Fig. 13 XRD patterns of lamellar mesostructured calcium phosphates prepared using (a) n-$C_8H_{17}NH_2$, (b) n-$C_{10}H_{21}NH_2$, (c) n-$C_{12}H_{25}NH_2$, (d) n-$C_{16}H_{33}NH_2$, and (e) n-$C_{18}H_{37}NH_2$

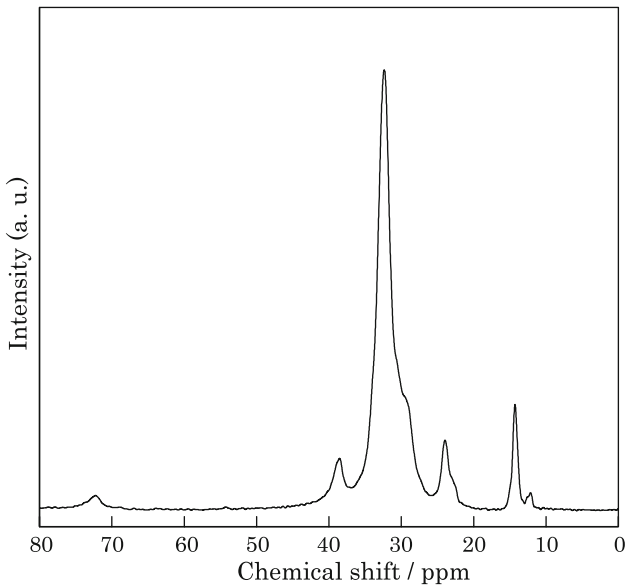

Fig. 14 ^{13}C CP/MAS NMR spectrum of lamellar mesostructured calcium phosphate obtained from the starting mixture of $Ca(OAc)_2$:H_3PO_4:n-$C_{16}H_{33}NH_2$:0.5NH_3:40EtOH:40H_2O

starting mixture with the composition of $Ca(OAc)_2$:H_3PO_4:n-$C_{16}H_{33}NH_2$:0.5NH_3:40EtOH:40H_2O is shown in Fig. 14. Several peaks due to carbon atoms in

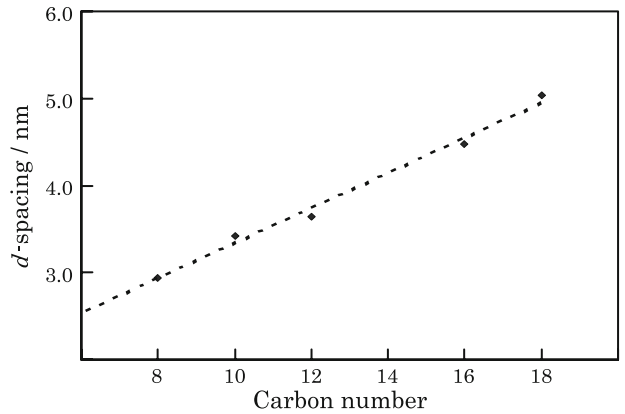

Fig. 15 Relationship between *d*-spacing and carbon number in the alkyl chain of *n*-alkylamine

n-$C_{16}H_{33}NH_2$ were observed and the peak at 32 ppm can be assigned to carbon atoms in all-*trans* methylene (–CH_2–) chains [52, 53]. Figure 15 shows the relation between the d_{001} spacing and the number of carbon atoms in the alkyl chains of *n*-$C_nH_{2n+1}NH_2$. In accordance with the correlation, a slope of the straight line is calculated to be 0.185 nm/CH_2. Since the distance between two adjacent carbon atoms are expressed as 0.127 nm/CH_2 in an all-*trans* alkyl chains [54], the alkyl chains are arranged in the lamellar phases as double layers with a tilt angle of ca. 46°. The wall thickness of the mesostructured calcium phosphates was estimated to be ca. 1.2 nm.

Conclusions

Lamellar mesostructured calcium phosphates constructed through ionic bonds were successfully synthesized by using *n*-$C_nH_{2n+1}NH_2$ as structure-directing agents. Lamellar mesostructured calcium phosphates was morphologically controlled by changing the alkyl chain length of aliphatic alcohols used as co-solvents. It is mainly important for the synthesis of lamellar mesostructured calcium phosphates to control both the solubility of calcium sources and the crystallization of calcium phosphate species. The controlled synthesis is possible in the mixed solvent systems of aliphatic alcohols and water that allows the interaction between the surfactant molecules and calcium phosphate species and the suppression of the discrete crystallization of calcium phosphate species. The calcium phosphate materials are promising as biomaterials such as bone prosthesis and adsorbents for biomolecules, and the crystallization and solubility controlled synthesis will open the new route to obtain mesostructured materials whose frameworks are constructed by ionic bonds.

References

1. Yanagisawa T, Shimizu T, Kuroda K, Kato C (1990) Bull Chem Soc Jpn 63:988. doi:10.1246/bcsj.63.988
2. Inagaki S, Fukushima Y, Kudoda K (1993) J Chem Soc Chem Commun 680. doi:10.1039/c39930000680
3. Kresge CT, Leonowicz ME, Roth WJ, Vartuli JC, Beck JS (1992) Nature 359:710. doi:10.1038/359710a0
4. Beck S, Vartuli JC, Roth WJ, Leonowicz ME, Kresge CT, Schmitt KD, Chu CT-W, Olson DH, Sheppard EW, McCullen SB, Higgins JB, Schlenker JL (1992) J Am Chem Soc 114:10834. doi:10.1021/ja00053a020
5. Zhao D, Feng L, Huo Q, Melosh N, Fredrickson GH, Chmelka BF, Stucky GD (1998) Science 279:548. doi:10.1126/science.279.5350.548
6. Zhao XS, Lu GQ, Millar GJ (1996) Ind Eng Chem Res 35:2075. doi:10.1021/ie950702a
7. Selvam P, Bhatia SK, Sonwane CG (2001) Ind Eng Chem Res 40:3237. doi:10.1021/ie0010666
8. Sayari A (1996) Chem Mater 8:1840. doi:10.1021/cm950585±
9. Corma A (1997) Chem Rev 97:2373. doi:10.1021/cr960406n
10. Taguchi A, Schüth F (2005) Micropor Mesopor Mater 77:1. doi:10.1016/j.micromeso.2004.06.030
11. Schüth F (2003) Angew Chem Int Ed 42:3604. doi:10.1002/anie.200300593
12. Monma H (1995) Inorg Mater 2:401
13. Rodriguez-Lorenzo LM, Vallet-Regi M (2000) Chem Mater 12:2460. doi:10.1021/cm001033g
14. Uota M, Arakawa H, Kitamura N, Yoshimura T, Tanaka J, Kijima T (2005) Langmuir 21:4724. doi:10.1021/la050029m
15. Vallet-Regí M, Ruiz-González L, Izquierdo-Barba I, González-Calbet JM (2006) J Mater Chem 16:26. doi:10.1039/b509744d
16. Huo Q, Leon R, Petroff PM, Stucky GD (1995) Science 268:1324. doi:10.1126/science.268.5215.1324
17. Huo Q, Margolese DI, Stucky GD (1996) Chem Mater 8:1147. doi:10.1021/cm960137h
18. Behrens P (1996) Angew Chem Int Ed 35:515. doi:10.1002/anie.199605151
19. Sayari A, Liu P (1997) Micropor Mater 12:149. doi:10.1016/S0927-6513(97)00059-X
20. Schüth F (2001) Chem Mater 13:3184. doi:10.1021/cm011030j
21. Tiemann M, Fröba M (2001) Chem Mater 13:3211. doi:10.1021/cm0110371
22. Kimura T (2005) Micropor Mesopor Mater 77:97. doi:10.1016/j.micromeso.2004.08.023
23. Yu C, Tian B, Zhao D (2003) Curr Opin Solid State Mater Sci 7:191. doi:10.1016/j.cossms.2003.10.004
24. Gao Q, Xu R, Chen J, Li R, Li S, Qui S, Yue YJ (1997) Chem Mater 9:457. doi:10.1021/cm9602611
25. Kimura T, Sugawara Y, Kuroda K (1999) Chem Mater 11:508. doi:10.1021/cm981036h
26. Mal NK, Fujiwara M, Ichikawa S, Kuraoka K (2002) J Ceram Soc Jpn 110:890
27. Mal NK, Ichikawa S, Fujiwara M (2003) Chem Commun 872. doi:10.1039/b300323j
28. Roca M, Haskouri JE, Cabrera S, Beltrán-Porter A, Alamo J, Beltrán-Porter D, Macros MD, Amorós P (1998) Chem Commun 1883. doi:10.1039/a803896a
29. Dasgupta S, Agarwal M, Datta A (2002) J Mater Chem 12:162. doi:10.1039/b109472f
30. Jiménez-Jiménez J, Maireles-Torres P, Olivera-Pastor P, Rodríguez-Castellón E, Jiménez-López A, Jones DJ, Rozière J (1998) Adv Mater 10:812. doi:10.1002/(SICI)1521-4095(199807)10:10≤812::AID-ADMA812≥3.0.CO;2-A

31. Jones DJ, Aptel G, Brandhorst M, Jacquin M, Jiménez-Jiménez J, Jiménez-López A, Maireles-Torres P, Piwonski I, Rodríguez-Castellón E, Zajac J, Rozière J (2000) J Mater Chem 10:1957. doi:10.1039/b002474k
32. Bhaumik A, Inagaki S (2001) J Am Chem Soc 123:691. doi:10.1021/ja002481s
33. Guo X, Ding W, Wang X, Yan Q (2001) Chem Commun 709. doi:10.1039/b100630o
34. Chang J-S, Park S-E, Gao Q, Férey G, Cheetham AK (2001) Chem Commun 859. doi:10.1039/b009160j
35. Tarafdar A, Biswas S, Pramanik NK, Pramanik P (2006) Micropor Mesopor Mater 89:204. doi:10.1016/j.micromeso.2005.10.027
36. Mal NK, Ichikawa S, Fujiwara M (2002) Chem Commun 112. doi:10.1039/b109948e
37. Ozin GA, Varaksa N, Coombs N, Davies JE, Perovic DD, Ziliox M (1997) J Mater Chem 7:1601. doi:10.1039/a702416i
38. Soten I, Ozin GA (1999) J Mater Chem 9:703. doi:10.1039/a806045b
39. Yao J, Tjandra W, Chen YZ, Tam KC, Ma J, Soh B (2003) J Mater Chem 13:3053. doi:10.1039/b308801d
40. Schmidt SM, McDonald J, Pineda ET, Verwilst AM, Chen Y, Josephs R, Ostefin AE (2006) Micropor Mesopor Mater 94:330. doi:10.1016/j.micromeso.2006.04.006
41. Tokuoka Y, Ito Y, Kitahara K, Niikura Y, Ochiai A, Kawashima N (2006) Chem Lett 35:1220. doi:10.1246/cl.2006.1220
42. Zhao YF, Ma J (2005) Micropor Mesopor Mater 87:110. doi:10.1016/j.micromeso.2005.07.046
43. Ikawa N, Oumi Y, Kimura T, Ikeda T, Sano T (2006) Chem Lett 35:948. doi:10.1246/cl.2006.948
44. Eanes ED, Gillessen IH, Posner AS (1965) Nature 208:365. doi:10.1038/208365a0
45. Oliver SRJ, Ozin GA (1998) J Mater Chem 8:1081. doi:10.1039/a708598b
46. Sivakumar GR, Girija EK, Karukura SN, Subramanian C (1998) Cryst Res Technol 33:197. doi:10.1002/(SICI)1521-4079(1998)33:2≤197::AID-CRAT197≥3.0.CO;2-K
47. Larson MJ, Thorsen A, Jensen SJ (1985) Calcif Tissue Int 37:189. doi:10.1007/BF02554840
48. Kim S, Ryu HS, Shin H, Jung HS, Hong KS (2005) Mater Chem Phys 91:500. doi:10.1016/j.matchemphys.2004.12.016
49. Aue WP, Roufosse AH, Glimcher MJ, Griffin RG (1984) Biochemistry 23:6110. doi:10.1021/bi00320a032
50. Miquel JL, Facchini L, Legrand AP, Rey C, Lemaitre J (1990) Colloids Surfaces 45:427. doi:10.1016/0166-6622(90)80041-2
51. Furuichi K, Oaki Y, Imai H (2006) Chem Mater 18:229. doi:10.1021/cm052213z
52. Simonutti R, Comotti A, Bracco S, Sozzani P (2001) Chem Mater 13:771. doi:10.1021/cm001088i
53. Kooli F, Mianhui L, Alshahateet SF, Chen F, Yinghuai Z (2006) J Phys Chem Solids 67:926. doi:10.1016/j.jpcs.2006.01.005
54. Kitaigorodskii AI (1973) Molecular crystals and molecules. Academic Press, New York